

Cite this: *RSC Adv.*, 2019, **9**, 22900

Influence of air contamination during heat-assisted plasma treatment on adhesion properties of polytetrafluoroethylene (PTFE)†

Yuji Ohkubo, * Tetsuya Nakagawa, Katsuyoshi Endo and Kazuya Yamamura

Plasma surface treatment is typically not effective on fluoropolymers containing polytetrafluoroethylene (PTFE). It is reported that heat-assisted plasma (HAP) treatment at high temperatures (above 200 °C) under atmospheric pressure helium (He) plasma improves the adhesion properties of PTFE. In this study, we investigated the influence of the air concentration during HAP treatment on the adhesion properties of PTFE. Air concentration was controlled via ambient air inflow amount, in other words, base pressure. The PTFE samples HAP-treated in different air concentrations were thermally compressed with an unvulcanized isobutylene-isoprene rubber (IIR). Then, the PTFE/IIR adhesion strength was measured via T-peel test. We show that, when PTFE was HAP-treated in 0.01% air, its PTFE/IIR adhesion strength was over 2 N mm⁻¹; the IIR underwent cohesion failure. However, the PTFE/IIR adhesion strength drastically decreased in the presence of air contamination. The relationships between air concentration during HAP treatment, adhesion properties of PTFE, surface chemical composition, surface morphology, and surface hardness were investigated and discussed.

Received 8th March 2019
Accepted 12th July 2019

DOI: 10.1039/c9ra01789e
rsc.li/rsc-advances

Introduction

Plasma can be artificially generated and applied in many surface engineering fields for three main purposes: surface modification, surface etching, and surface coating. Surface modification using plasma is applied for cleaning metal and glass surfaces, improving the wettability of ink or paint on a substrate, and enhancing the adhesion properties of polymers. For the past 50 years, plasma has been used as a pre-treatment to enhance the adhesion properties of several kinds of polymers such as polyethylene (PE), polypropylene (PP), polystyrene (PS), polyethylene terephthalate (PET), polyamide (PA), polyether ether ketone (PEEK), poly methyl methacrylate (PMMA), cyclo olefin polymers (COPs), liquid crystal polymers (LCPs), polydimethylsiloxane (PDMS), and polyimide (PI).^{1–9} In addition, plasma has been used to enhance the adhesion strength between composite materials such as carbon-fiber-reinforced plastics (CFRP) and wood-plastic composites.^{10,11} However, plasma treatment has little effect on polytetrafluoroethylene (PTFE) which is a representative fluoropolymer.^{12–14} As an alternative to impart adhesion properties to PTFE, surface graft polymerization can be applied during plasma treatment^{15,16} and after plasma treatment.^{17–19} On the other hand, our research group proposed a heat-assisted plasma (HAP)

treatment for the improvement of the adhesion properties of PTFE. HAP treatment involves applying heat to the PTFE surface by plasma treatment to induce surface hardening and introduce oxygen-containing functional groups.^{20,21} HAP treatment has been shown to effectively improve both the indirect adhesion using an adhesive and direct adhesion (without an adhesive) of PTFE to other materials.²²

However, the HAP treatment in the previous studies was a leaf-type process: the pressure in the chamber was reduced to below 10 Pa using a rotary vacuum pump, and helium (He) gas was subsequently flowed into the chamber until it reached atmospheric pressure (101 300 Pa).^{20–22} Thus, although the HAP treatment was conducted at atmospheric pressure, it was not an open-air-type plasma treatment, which limits the process throughput. Therefore, the throughput of the HAP treatment is low. To transition from the conventional HAP treatment in an evacuated chamber to open-air-type HAP treatment, the inflow of air must be considered. There are some reports of OH and NO_x production due to the inflow of ambient air and the occurrence of the shielding gas effect, which prevents the inflow of ambient air, during open-air-type plasma treatment.^{23–25} Other studies have compared the effectiveness of different plasma gas species, such as air and N₂, for plasma treatment of PE.^{26,27} However, the effects of air contamination on the plasma treatment (including HAP) of fluoropolymers have not been reported. Therefore, in this study, the influence of air contamination on the adhesion properties of a representative fluoropolymer, PTFE, was examined as the first step in the potential development of open-air-type HAP plasma treatment.

Graduate School of Engineering, Osaka University, 2-1 Yamadaoka, Suita, Osaka 565-0871, Japan. E-mail: okubo@upst.eng.osaka-u.ac.jp

† Electronic supplementary information (ESI) available. See DOI: [10.1039/c9ra01789e](https://doi.org/10.1039/c9ra01789e)



Experimental

Materials

Rolled PTFE sheets of 0.2 mm in thickness (NITOFLON® no. 900UL, Nitto Denko, Japan) were cut to dimensions of 70 mm \times 45 mm \times 0.2 mm. The PTFE sheets were washed with acetone (99.5%, Kishida Chemical, Japan) and then with pure water in an ultrasonic bath (US-4R, AS-ONE, Japan) for 1 min. The washed PTFE sheets were dried using pressurized N₂ gas (99.99%, Iwatani Fine Gas, Japan).

As an adherend for PTFE, isobutylene-isoprene rubber (IIR) was selected. IIR has higher gas permeability and higher weather resistance than other rubbers. Therefore, IIR is used as gasket material for a syringe prefilled with medical agents. IIR needs to be coated strongly with a PTFE sheet without using adhesives because IIR has low sliding property. In this study, unvulcanized IIR sheets of approximately 2 mm in thickness were prepared as previously described.²⁸ The IIR sheets were not washed before use.

Heat-assisted plasma (HAP) treatment method

It was previously reported that plasma treatment at low temperature (below 100 °C) has a little effect on the adhesion property of PTFE and HAP treatment (above 200 °C) has a significant effect on its adhesion property.^{20–22} Thus, the surface of each PTFE sheet was modified *via* HAP treatment according to the protocol reported previously.²¹ However, in this study, the air concentration was controlled by the base pressure (as shown in ESI-1†) during the HAP treatment. Before the HAP treatment, the pressure in a custom-made plasma reactor (Meisyo Kiko, Japan)^{20–22} was decreased using a rotary vacuum pump (GDH-361, Shimadzu, Japan). Then, helium (He) gas (99.99%, Iwatani Fine Gas, Japan) was flowed into the reactor until it reached atmospheric pressure (101 300 Pa). When the base pressure was 10, 500, and 2000 Pa, the calculated air concentration was 0.01%, 0.5%, and 2.0%, respectively. The applied power density for plasma generation was 19.1 W cm⁻², and the plasma treatment was carried out for 600 s according to the protocol reported previously.²⁹ During the treatment, the surface temperature of each PTFE sample during HAP treatment was measured using a digital radiation thermometer (FT-H40K and FT-50A, Keyence, Japan) to confirm that the maximum surface temperature remained above 200 °C.

To confirm the air inflow, optical emission spectroscopy (OES) was conducted using a multichannel spectrometer (HR-4000CG-UV-NIR, Ocean Optics, USA) and a light fiber (P400-2-VIS/NIR, Ocean Optics, USA). The measurement range was 200–1000 nm, and the measurement period was 3 s. Fig. 1 shows the OES spectra of PTFE samples following HAP treatments in different air concentrations. The peaks were identified using references as follows:^{24,30} peaks attributed to OH were observed at 309 nm, peaks corresponding to nitrogen (N₂) were observed at 330–380 and 390–430 nm, peaks attributed to oxygen (O) were observed at 777 and 845 nm, and peaks indexed to helium (He) were observed at 587, 667, 706, and 728 nm. The gas compositions were then calculated from the ratio of each

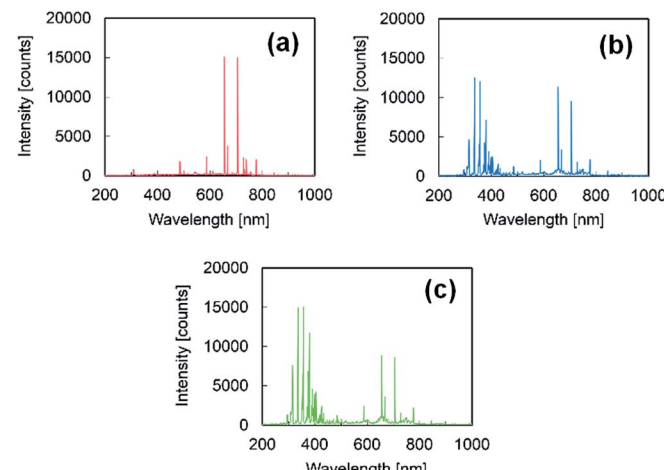


Fig. 1 OES spectra following HAP treatments in different air concentrations: (a) 0.01%, (b) 0.5%, and (c) 2.0%. Each measurement period was 3 s.

peak intensity relative to the intensity of the He peak at 706 nm. The ratios of OH (at 309 nm), N₂ (at 337 nm), and O (at 777) increased with increasing base pressure (ESI-2†). Thus, it was confirmed that the air concentration in the He atmosphere for conducting the HAP treatment could be controlled by adjusting the base pressure, which would further control the inflow of ambient air.

Adhesion strength measurements

The samples were prepared for the adhesion test between PTFE and IIR as previously reported.²⁹ Briefly, each HAP-treated PTFE sample was placed on an unvulcanized IIR sheet within a mold without an adhesive. Then, the PTFE/IIR assembly was thermally compressed under 10 MPa at 180 °C for 10 min using a hot-pressing machine (AH-2003, AS-ONE, Japan). The PTFE/IIR adhesion strength was measured by a T-peel test using a digital force gauge (ZP-200N, Imada, Japan) and an electronically driven stand (MX-500N, Imada, Japan). The average adhesion strength was calculated by dividing the average tensile strength by the width of the PTFE sample (about 10 mm). All trials were done in triplicate, and the average adhesion strength was calculated from the three measured values.

X-ray photoelectron spectroscopy (XPS)

The chemical composition of a polymer's surface changes upon plasma treatment. XPS was conducted using an XPS spectrometer (Quantum 2000, ULVAC-PHI, Japan) attached to an Al-K α X-ray source. The X-ray irradiation area was ϕ 100 μ m, and the take-off angle was 45°. During the XPS measurement, the sample was irradiated by a low-speed electron beam and an Ar ion beam to achieve charge neutralization. A narrow-scan XPS spectrum of C1s was recorded at 275–300 eV with a pass energy of 23.50 eV and a step size of 0.05 eV. Three measurements were performed for each PTFE sample before and after HAP treatment. The spectra were referenced to peaks indexed to $-\text{CF}_2-$ at



292.5 eV for as-received PTFE^{31,32} and 291.8 eV for plasma-treated PTFE.^{33,34}

Surface morphology observation

It is generally known that the polymer surface is etched because of plasma treatment, and as a result, the surface morphology changes. Thus, the micrometer-scale surface morphologies of the PTFE samples were observed before and after HAP treatment using scanning electron microscopy (SEM, JCM-6000, JEOL, Japan). Prior to SEM observation, a thin gold film was applied to each PTFE sample using an ion-sputtering apparatus (Smart Coater DII-29010SCTR, JEOL, Japan) to prevent electrification of the samples.

Etching rate measurements

It is predicted that the sample weight will decrease when the polymer surface is etched during HAP treatment. This weight loss was quantified by weighing the PTFE samples before and after plasma treatment using a high-accuracy electronic balance (HR202i, A&D Company, Japan) with a resolution of 0.1 mg. The etching rate was calculated by dividing the average weight loss by the area of the treated surface (34 mm × 30 mm) and the total treatment time (1800 s); thus, the etching rate was expressed in [$\mu\text{g cm}^{-2} \text{ s}^{-1}$]. More than three samples treated under each condition were evaluated, and the average weight loss of the three samples was used to calculate the average etching rate.

Surface hardness test

It is predicted that the HAP treatment will also alter the surface hardness of the PTFE. To quantify this effect, the load-depth curves of the as-received and plasma-treated PTFE samples were recorded at 20 ms intervals using a nanoindenter (ENT-2100, Elionix, Japan). The loading was controlled *via* electromagnetic force. The rate of loading was set at 1 $\mu\text{N}/250 \text{ ms}$, and the maximum loading was fixed at 40 μN . The displacement was measured *via* an optical displacement meter. Oliver and Pharr type was applied as a calibration method for an indenter tip. The indentation hardness was calculated by dividing the maximum load by the projected contact area. The indentation hardness was measured from over 50 different points on each PTFE sample, and the data were compiled into histograms. The average surface hardness was calculated as a geometric mean value of over 50 indentation hardness measurements.

Results and discussion

External appearance and adhesion strength

Before the thermal compression step, the change in the external appearance of the PTFE upon HAP treatment was visually observed. Fig. 2 shows the photographs of PTFE samples without HAP treatment and those with HAP treatments in different air concentrations. The PTFE samples treated by HAP in 0.01% and 0.5% air did not undergo externally visible changes when compared to the as-received PTFE (Fig. 2a–c). However, the PTFE treated by HAP in 2.0% air became more

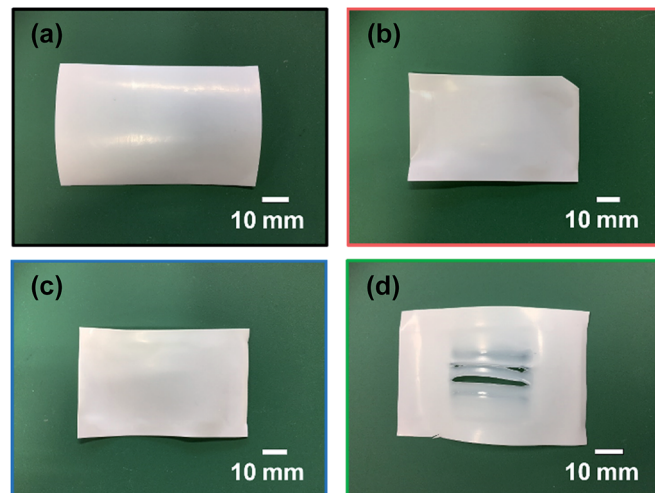


Fig. 2 Photographs of the PTFE samples without or with HAP treatments in different air concentrations: (a) as-received, (b) HAP-treated in 0.01% air, (c) HAP-treated in 0.5% air, and (d) HAP-treated in 2.0% air.

transparent and fractured (Fig. 2d), thus, it was clear that the 2.0% air condition resulted in significant different surface properties compared to those treated in 0.01% and 0.5% air and that 2.0% air is not practical for HAP treatment. For PTFE samples that were HAP-treated in 2.0% air, the parts in which no fracture was observed was used for the adhesion testing, XPS measurements, and surface hardness evaluation.

Fig. 3a shows the PTFE/IIR adhesion strengths of PTFE samples without or with HAP treatments in different air concentrations. The PTFE/IIR adhesion strength of the as-received PTFE sample was too low to measure (reported as 0.00 N mm⁻¹). However, the PTFE/IIR adhesion strength of the PTFE sample that was HAP-treated in 0.01% air was above 2 N mm⁻¹; in fact, the adhesion was so strong that cohesion failure occurred in the IIR during the T-peel test (Fig. 3b). When the PTFE sample was HAP-treated in 0.005% air, the PTFE/IIR adhesion strength was also above 2 N mm⁻¹ (as not shown in

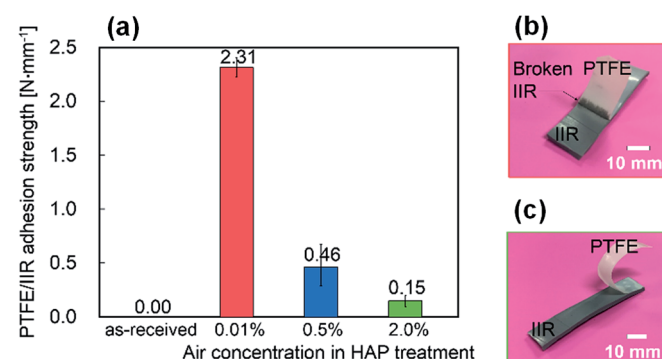


Fig. 3 Adhesion properties of the PTFE samples without or with HAP treatments in different air concentrations: (a) PTFE/IIR adhesion strengths, (b) photograph of the PTFE/IIR assembly with the PTFE sample that was HAP-treated in 0.01% air, and (c) photograph of the PTFE/IIR assembly with the PTFE sample that was HAP-treated in 2.0% air.



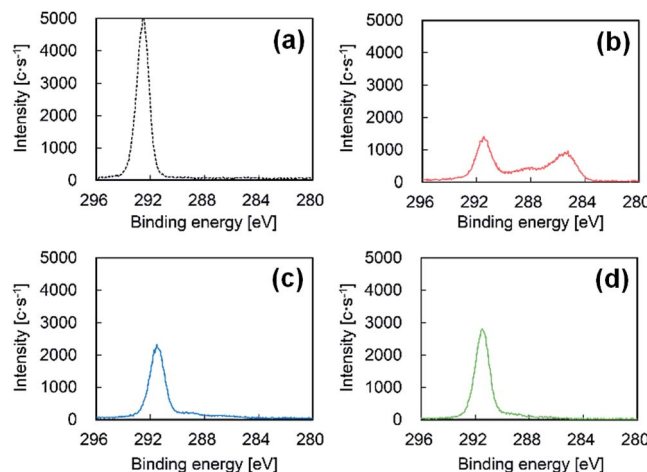


Fig. 4 C1s-XPS spectra of the PTFE samples without or with HAP treatments in different air concentrations: (a) as-received, (b) HAP-treated in 0.01% air, (c) HAP-treated in 0.5% air, and (d) HAP-treated in 2.0% air.

Fig. 3). These results indicate that the HAP treatment at low air concentration was effective for improving the adhesion property of PTFE. However, the PTFE/IIR adhesion strength of HAP-treated PTFE decreased with increasing air concentration during the treatment. With 0.5% air, the PTFE/IIR adhesion strength was drastically decreased, and when the air concentration was 2.0%, the HAP-treated PTFE was easily peeled off from the IIR (Fig. 3c). These results indicate that the HAP treatment at high air concentration was not effective for improving the adhesion property of PTFE. In short, it is critical to maintain a low air concentration during the HAP treatment in order to realize high adhesion strength.

Surface chemical composition

To clarify the reason why the PTFE/IIR adhesion strength of HAP-treated PTFE drastically decreased when treated in higher

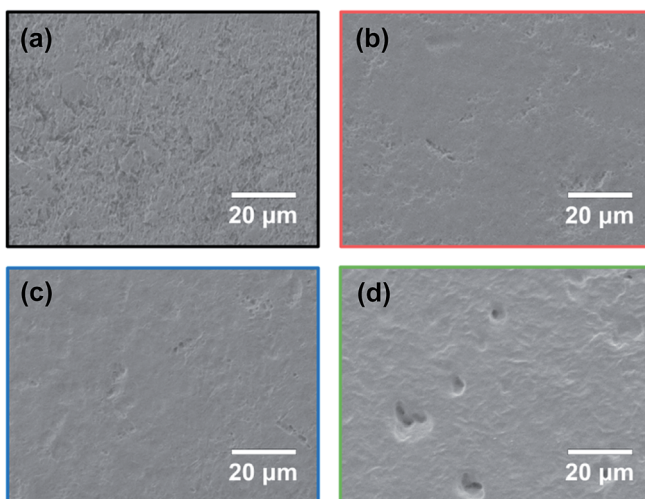


Fig. 5 SEM images of the PTFE samples without or with HAP treatments in different air concentrations: (a) as-received, (b) HAP-treated in 0.01% air, (c) HAP-treated in 0.5% air, and (d) HAP-treated in 2.0% air.

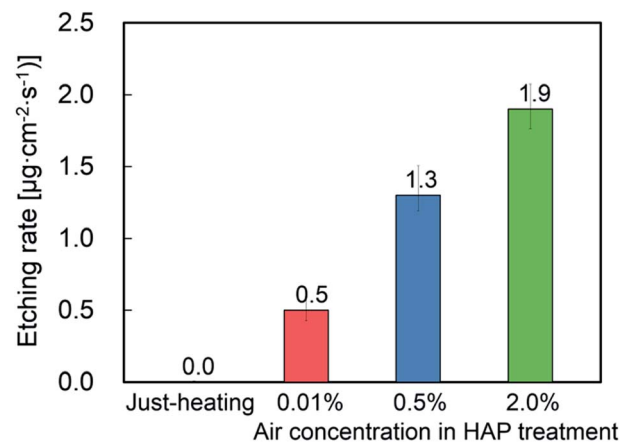


Fig. 6 Etching rates of the PTFE samples without or with HAP treatments in different air concentrations.

concentrations of air, the changes in the chemical composition of the surface upon HAP treatments were evaluated by XPS. Fig. 4 shows the C1s-XPS spectra of the PTFE samples without or with HAP treatments in different air concentrations. For the as-received PTFE, the only peak (292.5 eV) was indexed to CF_2 (Fig. 4a). However, for the PTFE sample treated by HAP in 0.01% air, the intensity of the CF_2 peak decreased, and peaks indexed to $\text{C}=\text{O}-\text{O}$ (289.0 eV), $\text{C}=\text{O}$ (288.2 eV), $\text{C}-\text{O}$ (286.5 eV), and $\text{C}-\text{C}$ (285.3 eV) appeared (Fig. 4b). By contrast, for the PTFE sample treated by HAP in 0.5% air, the intensities of the peaks indexed to $\text{C}=\text{O}-\text{O}$, $\text{C}=\text{O}$, $\text{C}-\text{O}$, and $\text{C}-\text{C}$ significantly decreased (Fig. 4c) compared to those in the PTFE treated by HAP in 0.01% air. Moreover, the C1s-XPS spectrum of the PTFE sample treated by HAP in 2.0% air approached that of the as-received PTFE (Fig. 4d). These results indicated that oxygen-containing functional groups were generated and $\text{C}-\text{C}$ crosslinking occurred

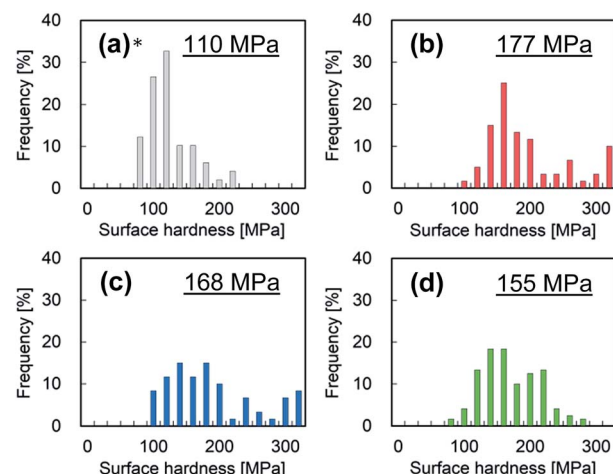


Fig. 7 Histograms of the surface hardness values of the PTFE samples without or with HAP treatments in different air concentrations: (a) as-received (*data measured in a previous study²¹), (b) HAP-treated in 0.01% air, (c) HAP-treated in 0.5% air, and (d) HAP-treated in 2.0% air. The underlined values denote the average surface hardness.

Table 1 Relation among air concentration, surface temperature, and the PTFE/IIR adhesion strength

Sample no.	Plasma	Air concentration	Temperature	Adhesion strength
As-received	No	—	—	0.00 N mm ⁻¹
1 ^a	Yes	0.01%	<100 °C	0.15 N mm ⁻¹
2 ^a	Yes	0.01%	<170 °C	1.28 N mm ⁻¹
3	Yes	0.01%	>200 °C	>2.0 N mm ^{-1c}
4	Yes	0.5%	>200 °C	0.46 N mm ⁻¹
5	Yes	2.0%	>200 °C	0.15 N mm ⁻¹
Just-heating ^b	No	0.01%	>200 °C	0.00 N mm ⁻¹

^a The data measured in a previous study.²⁰ ^b The data measured in a previous study.²¹ ^c Cohesion failure of IIR.

during the HAP treatment when the air concentration was 0.01% and did not occur when the air concentration was higher. Low adhesion strength can be correlated with the absence of oxygen-containing functional groups on the surface.

Surface morphology

It was previously reported that the presence of oxygen during plasma treatment enhances the etching of the PTFE surface.³⁵ Thus, it was predicted that the oxygen in the air would increase the etching of the PTFE surface during HAP. Fig. 5 shows the SEM images of PTFE samples without or with HAP treatments in different air concentrations. For the as-received PTFE, many cutting scratches and pits were observed (Fig. 5a), indicating the presence of a weak boundary layer (WBL) that is introduced to the PTFE surface during the cutting process as reported previously for other polymer surfaces.^{36,37} For the PTFE sample treated by HAP in 0.01% air, no cutting scratches and few pits were observed (Fig. 5b), indicating that the WBL was moderately removed *via* HAP treatment in a low air concentration. By contrast, crater-like holes were observed on the PTFE samples that were treated in higher air concentrations, but no cutting scratches were observed (Fig. 5c and d); moreover, the holes increased in diameter and depth with increasing air concentration. In addition, the surface roughness increased with increasing air concentration. Hubert *et al.* reported that the amorphous part of PTFE is more likely to be etched by atomic oxygen than the crystalline part, and therefore, an ultra-hydrophobic surface is created.³⁸ Thus, the roughened PTFE surfaces having crater-like holes are expected to inhibit strong adhesion.

Etching rate

The SEM images in Fig. 5 indicate that the HAP treatment etched the PTFE surface and removed the WBL. The degree of etching is quantified in ESI-3,† and the calculated etching rates of the HAP treatments in different air concentrations are shown in Fig. 6. For the PTFE that was only heated at 205 °C using a halogen heater without plasma treatment, the sample weight was unchanged, demonstrating that the PTFE surface was not etched because of heating alone. By contrast, the HAP treatments decreased the sample weight, indicating that the PTFE surface was etched because of the HAP treatment. In addition, the etching rate increased with increasing air concentration

during the HAP treatment. It was previously reported that, during plasma treatment, atomic oxygen preferentially etches amorphous PTFE and increases the surface roughness.³⁸ Another article reported that O₂ plasma induces more etching than other plasma gas species, including N₂, H₂, NH₃, and Ar.³⁹ The observed increase in etching with increasing air concentration (corresponding to increasing inflow of ambient air) is consistent with these previous findings. Considering these results with the surface chemical compositions, it can be concluded that excessive etching removes from the PTFE surface not only the original WBL but also the carbon radicals, oxygen-containing functional groups, and C–C crosslinkings that are generated *via* the HAP treatment, resulting in a surface that is similar to that of as-received PTFE. This theory also explains the decrease in the adhesion property of PTFE with increasing air concentration during HAP treatment.

Surface hardness

The representative load–depth curves of PTFE samples without or with HAP treatments in different air concentrations were shown in ESI-4,† Fig. 7 shows the histograms of the surface hardness values measured from the PTFE samples without or with HAP treatments in different air concentrations. The as-received PTFE sample had the lowest surface hardness (110 MPa). Although the surface hardness increased upon HAP treatment, the increase, compared to that of as-received PTFE (110 MPa), was less significant with increasing air concentration. This result implies that the presence of too much air during the HAP treatment, which promotes etching, also destroys the C–C crosslinking that is responsible for maintaining surface hardness. A similar relation between surface hardness and adhesion properties has been reported previously.²² Thus, the high surface hardness in the PTFE treated by HAP in 0.01% air in the present study may be another factor contributing to its high adhesion strength.

Conclusions

In this study, we examined the influence of air contamination during HAP treatment on the adhesion properties of PTFE. The air concentration was controlled to be 0.01%, 0.5%, and 2.0% by adjusting the base pressure before introducing helium (He) gas. The results show that the PTFE/IIR adhesion strength was over



2 N mm⁻¹ when the air concentration was very low (0.01%). However, the PTFE/IIR adhesion strength drastically decreased with increasing air concentration.

Furthermore, the relationships between the air concentration during HAP treatment and chemical composition, morphology, etching rate, and hardness of the PTFE surface were also investigated. The results showed that HAP treatment in 0.01% air induced surface hardening and introduction of oxygen-containing functional groups. In contrast, increasing the air concentration increases the etching rate, and this resulted in decreases in both the amount of oxygen-containing functional groups and the surface hardness, which were considered to be two factors contributing to the decrease in the adhesion property of PTFE. Furthermore, these results indicate that it is crucial to control air contamination during HAP treatment; only 0.5% air drastically decreases the resulting adhesion property of PTFE. In addition, the surface temperature during the plasma treatment must be maintained at more than 200 °C in order to realize strong adhesion because even if the air concentration during plasma treatment without heating is controlled to be low, such as 0.01% air, the adhesion property of PTFE does not improve.^{20–22} The relationship between air concentration, surface temperature, and PTFE/IIR adhesion strength was summarized at Table 1. In summary, we must pay attention to both the air concentration and surface temperature to attain the desirable effect of plasma treatment on the adhesion property of PTFE; controlling only one or the other factor is not effective.

Conflicts of interest

The authors declare no conflict of interest.

Acknowledgements

The IIR was provided gratis by Hyogo Prefectural Institute of Technology; we thank them for their assistance. In addition, we are also thankful to the Iketani Science and Technology Foundation (Grant No. 0281005-A) for their support of this research.

Notes and references

- 1 J. R. Hall, C. A. L. Westerdahl, A. T. Devine and M. J. Bodnar, *J. Appl. Polym. Sci.*, 1969, **13**, 2085–2096.
- 2 S. Hamdan and J. R. G. Evans, *J. Adhes. Sci. Technol.*, 1987, **1**, 281–289.
- 3 M. S. Shenton, M. C. Lovell-Hoare and G. C. Stevens, *J. Phys. D: Appl. Phys.*, 2001, **34**, 2754–2760.
- 4 H. Shinohara, J. Mizuno and S. Shoji, *Sens. Actuators, A*, 2001, **165**, 124–131.
- 5 H. Shinohara, J. Mizuno and S. Shoji, *IEEE Trans. Electr. Electron. Eng.*, 2007, **2**, 301–306.
- 6 S. Zhang, F. Awaja, N. James, D. R. McKenzie and A. J. Ruys, *Colloids Surf., A*, 2011, **374**, 88–95.
- 7 U. Alam, Y. Qin, M. R. Howlader and M. J. Deen, *RSC Adv.*, 2016, **6**, 107200–107207.
- 8 Y. Li and Y. C. Liao, *ACS Appl. Mater. Interfaces*, 2016, **8**, 11868–11874.
- 9 J. H. Kim, T. I. Lee, T. S. Kim and K. W. Paik, *IEEE Trans. Compon., Packag., Manuf. Technol.*, 2017, **7**, 1583–1591.
- 10 N. Metzler, K. Dantonello, M. Roßmeier, M. Bauer, S. Horn and M. Kupke, *J. Mater. Sci. Surf. Eng.*, 2016, **8**, 472–482.
- 11 J. Yáñez-Pacíos and J. M. Martín-Martínez, *Plasma Chem. Plasma Process.*, 2018, **38**, 871–886.
- 12 N. Inagaki, S. Tasaka and T. Umehara, *J. Appl. Polym. Sci.*, 1999, **7**, 2191–2200.
- 13 S. R. Kim, *J. Appl. Polym. Sci.*, 2000, **77**, 1913–1920.
- 14 V. Rodriguez-Santiago, A. A. Bujanda, B. E. Stein and D. D. Pappas, *Plasma Processes Polym.*, 2011, **8**, 631–639.
- 15 M. Okubo, M. Tahara, T. Kuroki, T. Hibino and N. Saeki, *J. Photopolym. Sci. Technol.*, 2008, **21**, 219–224.
- 16 M. Okubo, M. Tahara, Y. Aburatani, T. Kuroki and T. Hibino, *IEEE Trans. Ind. Appl.*, 2010, **46**, 1715–1721.
- 17 E. T. Kang and Y. Zhang, *Adv. Mater.*, 2000, **12**, 1481–1494.
- 18 M. C. Zhang, E. T. Kang, K. G. Neoh and K. L. Tan, *Colloids Surf., A*, 2001, **176**, 139–150.
- 19 L. Zhang, Y. Chen and T. Dong, *Surf. Interface Anal.*, 2004, **36**, 311–316.
- 20 Y. Ohkubo, K. Ishihara, H. Sato, M. Shibahara, A. Nagatani, K. Honda, K. Endo and K. Yamamura, *RSC Adv.*, 2017, **7**, 6432–6438.
- 21 Y. Ohkubo, K. Ishihara, M. Shibahara, A. Nagatani, K. Honda, K. Endo and K. Yamamura, *Sci. Rep.*, 2017, **7**, 9476.
- 22 Y. Ohkubo, M. Shibahara, A. Nagatani, K. Honda, K. Endo and K. Yamamura, *J. Adhes.*, 2019, DOI: 10.1080/00218464.2018.1512859.
- 23 V. Pipa, S. Reuter, R. Foest and K. D. Weltmann, *J. Phys. D: Appl. Phys.*, 2012, **45**, 085201.
- 24 S. Reuter, J. Winter, A. Schmidt-Bleker, H. Tresp, M. U. Hammer and K. D. Weltmann, *IEEE Trans. Plasma Sci.*, 2012, **40**, 2788–2794.
- 25 E. R. W. Van Doremaele, V. S. S. K. Kondeti and P. J. Bruggeman, *Plasma Sources Sci. Technol.*, 2018, **27**, 095006.
- 26 S. O'Kell, T. Henshaw, G. Farrow, M. Aindow and C. Jones, *Surf. Interface Anal.*, 1995, **23**, 319–327.
- 27 U. Lommatsch, D. Pasedag, A. Baumann, G. Ellinghorst and H. E. Wagner, *Plasma Processes Polym.*, 2007, **4**, S1041–S1045.
- 28 H. Nakano, Japan patent 5767528, 26 June 2015, J-Plat Pat, https://www.j-platpat.inpit.go.jp/web/PU/JPB_5767528/A0E7706779B69900134518459524470F.
- 29 Y. Ohkubo, M. Shibahara, A. Nagatani, K. Honda, K. Endo and K. Yamamura, *J. Adhes.*, 2019, **95**, 242–257.
- 30 F. Massines, R. Messaoudi and C. Mayoux, *Plasmas Polym.*, 1998, **3**, 43–59.
- 31 N. Vandecasteele and F. Reniers, *J. Electron Spectrosc. Relat. Phenom.*, 2010, **178–179**, 394–408.
- 32 J. Hubert, T. Dufour, N. Vandecasteele, S. Desbief, R. Lazzaroni and F. Reniers, *Langmuir*, 2012, **28**, 9466–9474.
- 33 Y. Momose, Y. Tamura, M. Ogino and S. Okazaki, *J. Vac. Sci. Technol., A*, 1992, **10**, 229–238.



34 D. J. Wilson, R. L. Williams and C. Mayoux, *Plasmas Polym.*, 1998, **3**, 385–396.

35 E. A. D. Carbone, N. Boucher, M. Sferrazza and F. Reniers, *Surf. Interface Anal.*, 2010, **42**, 1014–1018.

36 H. Schonhorn and R. H. Hansen, *J. Appl. Polym. Sci.*, 1967, **11**, 1461–1474.

37 J. J. Bikerman, *Ind. Eng. Chem.*, 1967, **59**, 40–44.

38 J. Hubert, J. Mertens, T. Dufour, N. Vandencasteele, F. Reniers, P. Viville, R. Lazzaroni, M. Raes and H. Terry, *J. Mater. Res.*, 2015, **21**, 3177–3191.

39 N. Inagaki, K. Narushima, N. Tuchida and K. Miyazaki, *J. Polym. Sci., Part B: Polym. Phys.*, 2004, **42**, 3727–3740.

